Journal of Experimental Nanoscience
Publication details, including instructions for authors and subscription information:
http://www.informaworld.com/smpp/title~content=t716100757

HRTEM and Raman characterisation of the onion-like carbon synthesised by annealing detonation nanodiamond at lower temperature and vacuum

Q. Zou[a]; M. Z. Wang[a]; Y. G. Li[a]; B. Lv[a]; Y. C. Zhao[a]
[a] State Key Laboratory of Metastable Materials Science and Technology, Yanshan University, Qinhuangdao 066004, Hebei, P.R. China

Online publication date: 17 December 2010

To cite this Article Zou, Q. , Wang, M. Z. , Li, Y. G. , Lv, B. and Zhao, Y. C.(2010) 'HRTEM and Raman characterisation of the onion-like carbon synthesised by annealing detonation nanodiamond at lower temperature and vacuum', Journal of Experimental Nanoscience, 5: 6, 473 — 487
To link to this Article: DOI: 10.1080/17458081003646982
URL: http://dx.doi.org/10.1080/17458081003646982

Journal of Experimental Nanoscience
Vol. 5, No. 6, December 2010, 473–487

Taylor & Francis
Taylor & Francis Group

HRTEM and Raman characterisation of the onion-like carbon synthesised by annealing detonation nanodiamond at lower temperature and vacuum

Q. Zou, M.Z. Wang*, Y.G. Li, B. Lv and Y.C. Zhao

State Key Laboratory of Metastable Materials Science and Technology, Yanshan University, Qinhuangdao 066004, Hebei, P.R. China

(*Received 23 June 2009; final version received 24 January 2010*)

Onion-like carbon (OLC) was synthesised by annealing detonation nanodiamond for 1.5 h at temperatures from 500 to 1400°C and at a vacuum of 1 Pa. The results showed that the nanodiamond was transformed into the amorphous carbon (a-C) at first and then the a-C was transformed into the OLC gradually with the increase in annealing temperature. Moreover, at the annealing temperature of 600°C, the nanodiamond started transforming into a-C from the edge of the nanodiamond particle (1 1 1) crystal plane. At the annealing temperature of 750°C, the nanodiamond was transformed into the a-C completely. At the annealing temperature of 850°C, the a-C began transforming into the OLC at the edge area. At the annealing temperature of 1000°C, the OLC particle with a size smaller than 5 nm was synthesised. However, in the centre of the OLC particle, untransformed a-C coexisted. At the annealing temperature of 1100°C, the microstructure of the OLC particle with a size smaller than 5 nm became optimised. At the annealing temperature of 1200°C, the OLC particle with a size larger than 5 nm was fabricated. There was also untransformed a-C coexisting in the centre of the OLC particle. At the annealing temperature of 1350°C, all the a-C was transformed into the OLC. The average size of the OLC was approximately 5 nm, which was the same as that of the nanodiamond. The layers of the OLC were varied from several to 12.

Keywords: onion-like carbon; nanodiamond; characterisation; annealing

1. Introduction

Onion-like carbon (OLC) is a larger cluster composed of concentric carbon shells with a number of atoms. The innermost layer of the OLC composes 60 carbon atoms, and the number of carbon atoms for the second and the third layers increases in terms of $60\,n^2$. The shell spacing of the OLC is typically 0.34 nm, which is close to that of the graphite. The innermost diameter of the OLC is approximately 0.7 nm, which is close to that of the C_{60} [1].

Since the discovery of the OLC, it has attracted wide attention due to its unique microstructures and broad prospects of application [2–12]. After years of experiments,

*Corresponding author. Email: 1465314@qq.com

ISSN 1745–8080 print/ISSN 1745–8099 online

DOI: 10.1080/17458081003646982
http://www.informaworld.com

a variety of new methods have been developed for synthesising the OLC, summarised in the following categories: arc discharge method [13–15], electron beam irradiation method [16–22], catalytic decomposition of carbon-containing material [23–27], heat treatment method [28–31], mechanical milling method [32,33], carbon ion beam implantation [34], detonation [35], radio frequency (rf) plasma and combustion synthesis [36], etc. Various OLCs composing the graphite layers from several to hundreds have been synthesised using the above methods, such as single OLC, hollow OLC and an OLC with a package of various metallic elements within it.

There are many types of methods and a wide range of raw materials for preparing the OLC. Theoretically, all the carbonaceous material can be transformed into the OLC through certain preparation methods. However, there are still many problems for synthesising the OLC, for example, low purity, high structural defect, low yield, high synthesis cost, etc. In particular, the high synthesis cost and low yield are not conducive to further research on its performances and applications. For example, the lowest annealing temperature and the vacuum reported are 1200°C and 1.0×10^{-2} Pa, respectively, for the heat treatment method [37–39]. These conditions are very difficult for realising volume-produce of the OLC, which limit the application of the OLC. Moreover, there are no reports on the transformation of the nanodiamond into the OLC completely, even at the annealing temperature of 1400°C. Therefore, new technologies and raw materials have to be constantly explored to reduce the synthesis cost and increase its output. The most important thing is that the mechanism for the transformation is not yet clear.

In this work, the OLC was synthesised by annealing detonation nanodiamond for 1.5 h in a lower vacuum of 1 Pa and at annealing temperatures from 500°C to 1400°C. The OLC as-synthesised was characterised comprehensively using a high-resolution transmission electron microscope (HRTEM) and a Raman spectrometer. At the same time, the mechanism for the OLC synthesis by annealing the nanodiamond, was discussed.

2. Experiments

The nanodiamond powder was fabricated by a method of explosion and post-treated with a hot mixture of concentrated H_2SO_4 and $HClO_4$ [40,41]. The average size of the nanodiamond particle was approximately 5 nm. However, its particle size varied in the range from 2 to 12 nm.

The OLC was synthesised by annealing the detonation nanodiamond powder in a carbon furnace, whose type was ZT-50-20 and was bought from China. At first, the nanodiamond powder was put in a graphite tube. Then, the graphite tube was placed in the furnace chamber. During the annealing experiment, the vacuum of the furnace chamber was kept at about 1 Pa and the annealing temperatures were changed from 500 to 1400°C. The heat preservation was 1.5 h for each annealing temperature. Finally, the annealed samples were cooled to room temperature in the vacuum chamber of the carbon furnace. Before heating, the furnace chamber was evacuated to approximately 1 Pa first by a mechanical pump and then by a diffusion pump with oil. However, a cold trap using liquid nitrogen was applied in the vacuum line between the pump and the furnace chamber preventing the oil from moving into the furnace vacuum chamber.

The nanodiamond and the OLC as-synthesised were characterised comprehensively using an HRTEM (JEM-2010, Japan) for observing their microstructures and a Raman spectrometer (E55 + FRA 106, Germany) for determining its content.

3. Results and discussion

Figure 1 shows the HRTEM image and the selected area diffraction (SAD) pattern of the nanodiamond used. From the HRTEM image shown in Figure 1(a), we can see that the shape of the nanodiamond particles was almost spherical. The average size of the nanodiamond particle was about 5 nm. Its particle size varied in the range from 2 to 12 nm. The SAD pattern of the nanodiamond shown in Figure 1(b) exhibits a circle comprised

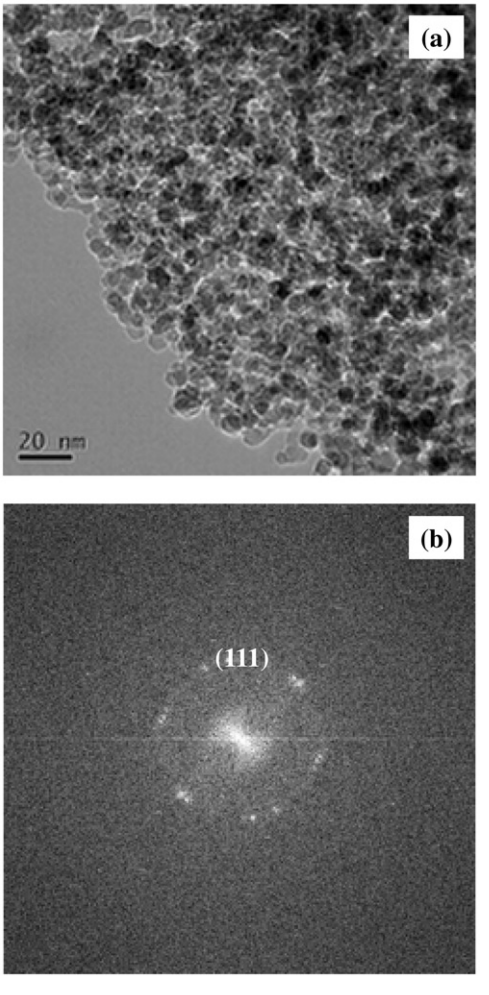

Figure 1. HRTEM image (a) and SAD pattern (b) of the nanodiamond.

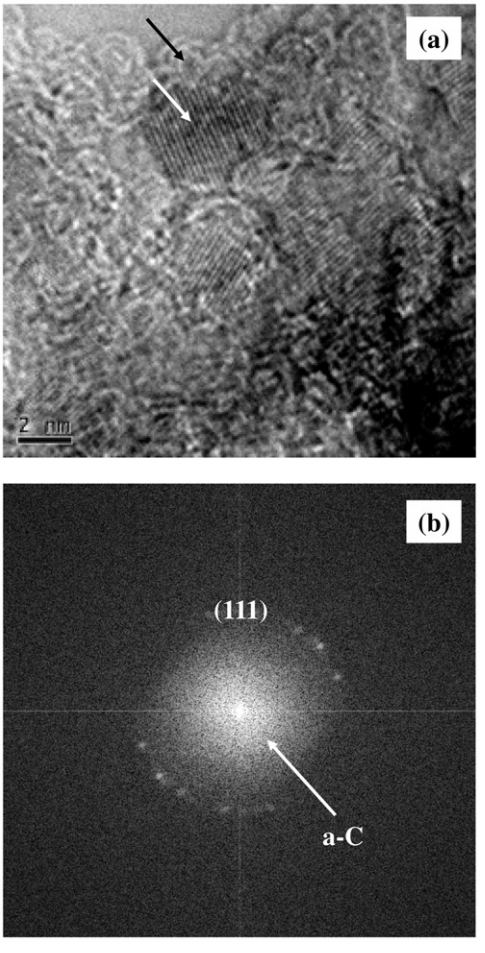

Figure 2. HRTEM image (a) and SAD pattern (b) of the nanodiamond annealed for 1.5 h at a temperature of 600°C.

of diffraction dots corresponding to the diffraction of the nanodiamond (1 1 1) crystal plane. This is a characteristic of detonation-synthesised nanodiamond particles [42,43].

Figure 2 shows the HRTEM image and the SAD pattern of the nanodiamond sample annealed for 1.5 h at the annealing temperature of 600°C in a vacuum of 1 Pa. At the annealing temperature of 600°C, the amorphous carbon (a-C) began appearing from the surface of the nanodiamond particles, as indicated by the white arrow in Figure 2(a). However, the (1 1 1) planes of the nanodiamond could be observed in the centre of the nanodiamond particles as indicated by the black arrow in Figure 2(a), which demonstrated that the centre of the nanodiamond particle was still diamond. Figure 2(b) shows the SAD pattern of the sample. The diffraction is composed of diffraction dots corresponding to the diffraction of the nanodiamond (1 1 1) plane, as shown in Figure 2(b). The centre area in the SAD pattern shown in Figure 2(b) corresponds to the diffraction of a-C. From the

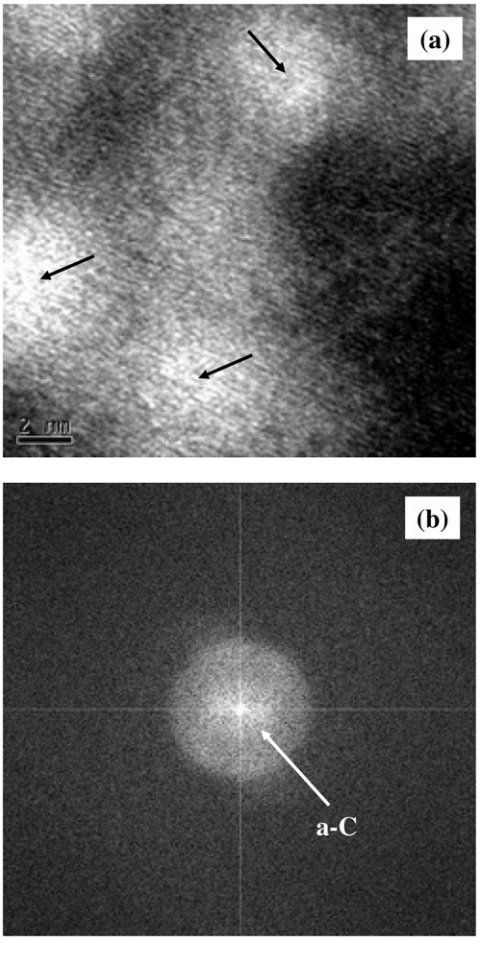

Figure 3. HRTEM image (a) and SAD pattern (b) of the nanodiamond annealed for 1.5 h at a temperature of 750°C.

SAD pattern of the sample shown in Figure 2(b), we can see that the a-C and the nanodiamond diffraction coexisted after annealing the nanodiamond at the condition. This agreed very well with the HRTEM image result shown in Figure 2(a).

Figure 3 shows the HRTEM image and the SAD pattern of the nanodiamond sample annealed for 1.5 h at the annealing temperature of 750°C in a vacuum of 1 Pa. The HRTEM image shown in Figure 3(a) indicates that the sample was arranged in the short range older as indicated by the black arrows. This suggested that almost all the nanodiamond particles were transformed into the a-C. The SAD pattern shown in Figure 3(b) indicates that the diffraction circle or arc composed of diffraction dots corresponding to the nanodiamond (1 1 1) crystal plane diffraction disappeared, in comparison to Figures 1(b) and 2(b). Only the a-C diffraction existed in the centre area of the SAD pattern. Furthermore, this suggested that all the nanodiamond particles were transformed into the a-C after annealing the nanodiamond in the condition.

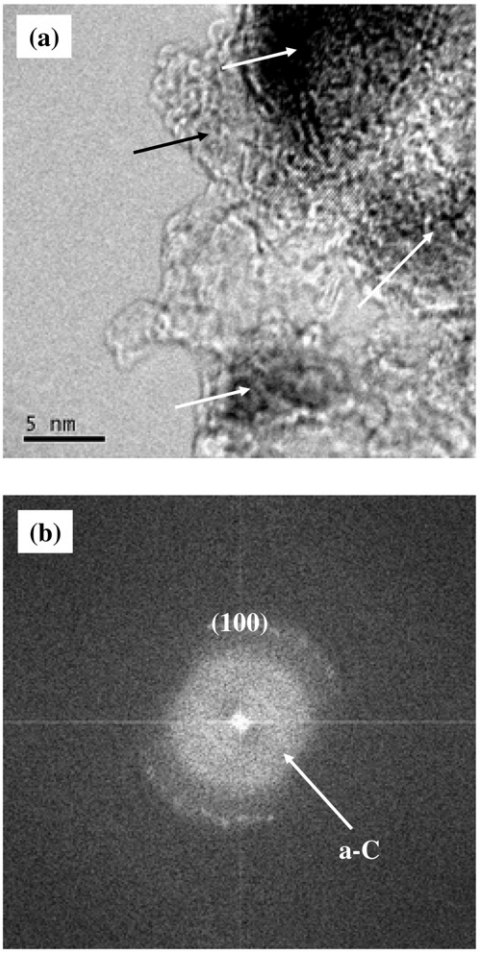

Figure 4. HRTEM image (a) and SAD pattern (b) of the nanodiamond annealed for 1.5 h at a temperature of 850°C.

Figure 4 shows the HRTEM image and the SAD pattern of the nanodiamond sample annealed for 1.5 h at the annealing temperature of 850°C in a vacuum of 1 Pa. From Figure 4(a), it can be clearly observed that the OLC fragments began appearing only at the edge, as indicated by the black arrow. There was untransformed a-C in the centre of the OLC fragments as indicated by the white arrows. However, there were no OLC particles observed after annealing the nanodiamond in the condition. The SAD pattern of the sample is shown in Figure 4(b). The diffraction arc composed of the diffraction dot in Figure 4(b) corresponds to the diffraction of the nanographite (1 0 0) plane. The centre area in the SAD pattern shown in Figure 4(b) corresponds to the diffraction of a-C. From the SAD pattern of the sample shown in Figure 4(b), we can see that the a-C and the nanographite diffraction coexisted after annealing the nanodiamond in the condition. This agreed very well with the HRTEM image result shown in Figure 4(a).

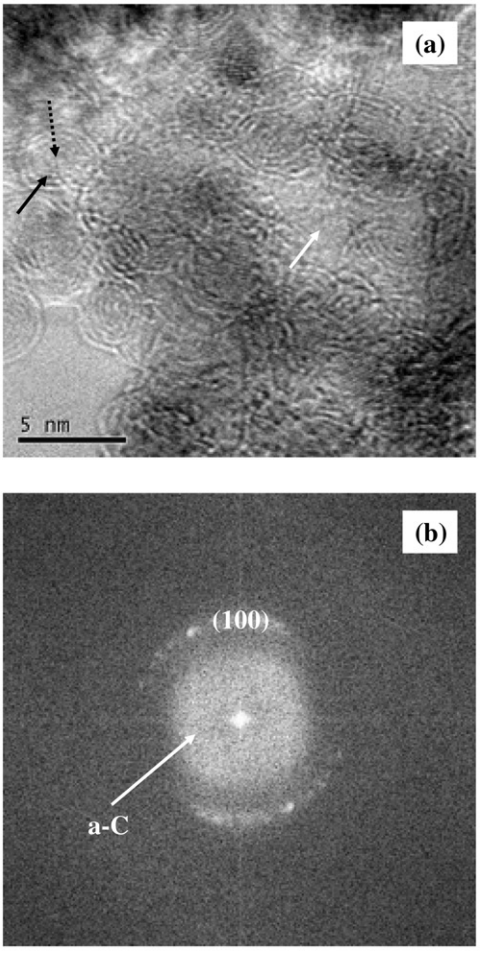

Figure 5. HRTEM image (a) and SAD pattern (b) of the nanodiamond annealed for 1.5 h at a temperature of 1000°C.

Figure 5 shows the HRTEM image and the SAD pattern of the nanodiamond sample annealed for 1.5 h at the annealing temperature of 1000°C in a vacuum of 1 Pa. Figure 5(a) shows that the OLC particles indicated by the black solid arrow coexisted with the untransformed a-C indicated by the white arrow. However, only the OLC particles with a size smaller than 5 nm were fabricated. Moreover, there was untransformed a-C existing in the centre of the OLC particle as indicated by the black dotted line arrow. Figure 5(b) shows the SAD pattern of the sample. The diffraction arc composed of the diffraction dot in Figure 5(b) corresponds to the diffraction of the nanographite (1 0 0) plane. The centre area in the SAD pattern shown in Figure 5(b) corresponds to the diffraction of a-C. From the SAD pattern of the sample shown in Figure 5(b), we can see that the a-C and the nanographite diffraction coexisted after annealing the nanodiamond in the condition. This agreed very well with the HRTEM image result shown in Figure 5(a).

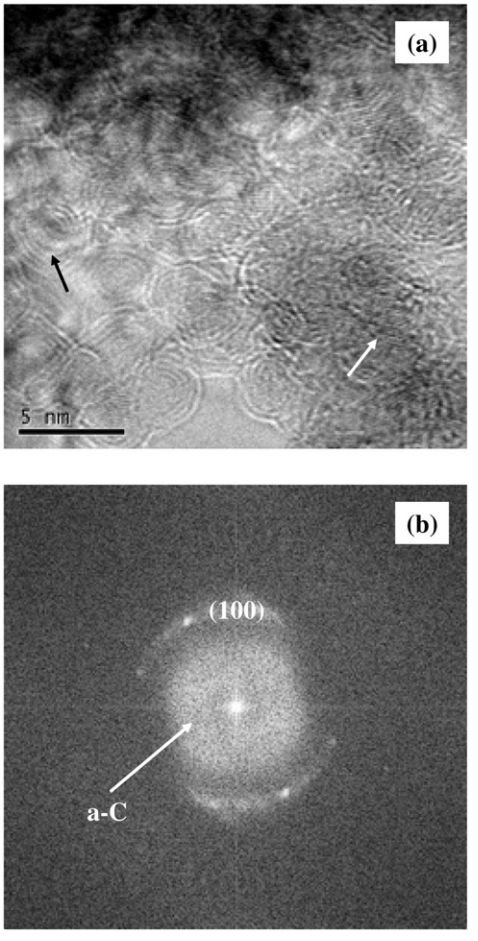

Figure 6. HRTEM image (a) and SAD pattern (b) of the nanodiamond annealed for 1.5 h at a temperature of 1100°C.

Figure 6 shows the HRTEM image and the SAD pattern of the nanodiamond sample annealed for 1.5 h at the annealing temperature of 1100°C in a vacuum of 1 Pa. Figure 6(a) shows that the OLC structure was optimised at the annealing temperature of 1000°C as indicated by the black arrow. Moreover, the OLC particles appeared with a larger size than that of annealed at the temperature of 1000°C as indicated by the white arrow. However, the OLC particle size was still smaller than 5 nm. Moreover, there was a-C coexisting in the centre of the OLC particles. Figure 6(b) shows the SAD pattern of the sample. The diffraction arc composed of the diffraction dot in Figure 6(b) and corresponds to the diffraction of the nanographite (1 0 0) plane. The centre area in the SAD pattern shown in Figure 6(b) corresponds to the diffraction of a-C. From the SAD pattern of the sample shown in Figure 6(b), we can see that the a-C and the nanographite diffraction coexisted after annealing the nanodiamond in the condition. This agreed very well with the HRTEM image result shown in Figure 6(a).

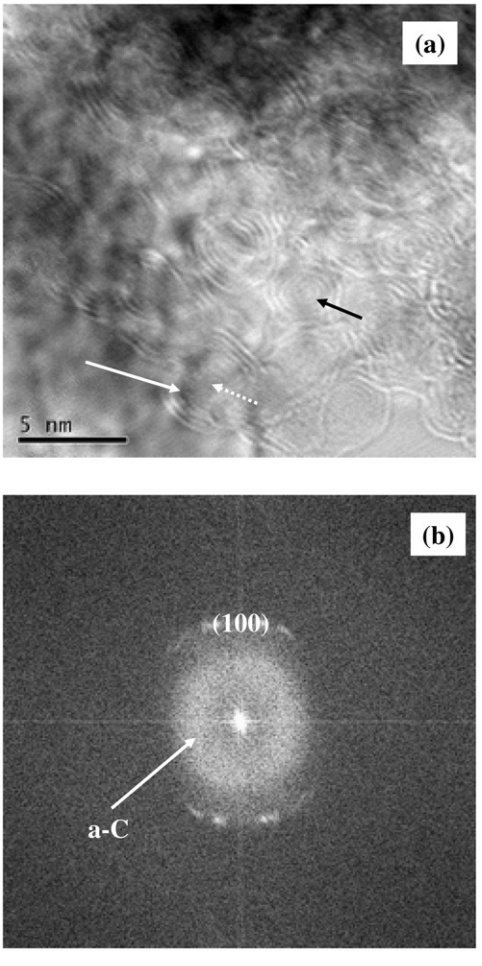

Figure 7. HRTEM image (a) and SAD pattern (b) of the nanodiamond annealed for 1.5 h at a temperature of 1200°C.

Figure 7 shows the HRTEM image and the SAD pattern of the nanodiamond sample annealed for 1.5 h at the annealing temperature of 1200°C in a vacuum of 1 Pa. Figure 7(a) shows the high magnification HRTEM image of the sample. From the HRTEM image, we can see clearly that the OLC particles with a size larger than 5 nm were synthesised, as indicated by the white solid arrow. However, there was untransformed a-C existing in the centre of the OLC particle. At the same time, the OLC particle with a size smaller than 5 nm, as indicated by the black arrow, became better than that of annealed at the temperature of 1100°C. Figure 7(b) shows the SAD pattern of the sample. The diffraction arc composed of the diffraction dot in Figure 7(b) corresponds to the diffraction of the nanographite (1 0 0) plane. The centre area in the SAD pattern shown in Figure 7(b) corresponds to the diffraction of a-C. From the SAD pattern of the sample shown in Figure 7(b), we can see that the a-C and the nanographite diffraction coexisted after

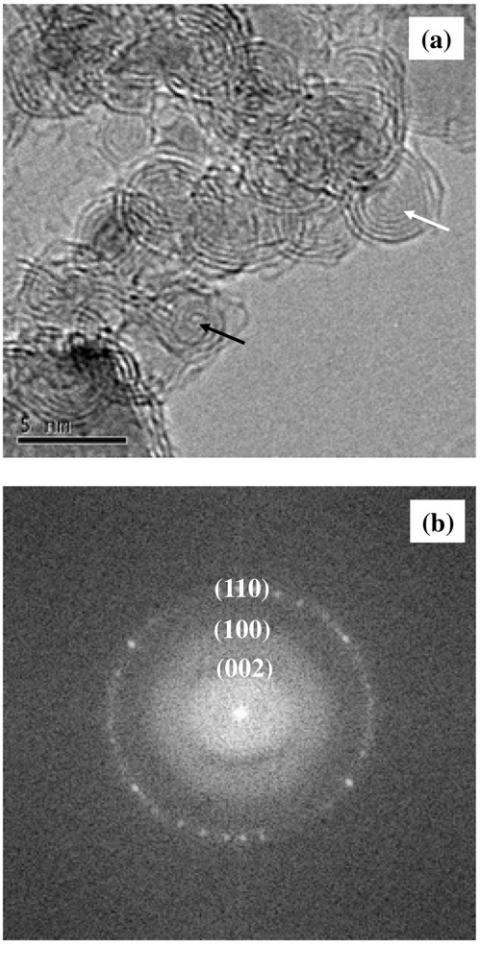

Figure 8. HRTEM image (a) and SAD pattern (b) of the nanodiamond annealed for 1.5 h at a temperature of 1350°C.

annealing the nanodiamond in the condition. This agreed very well with the HRTEM image result shown in Figure 7(a).

Figure 8 shows the HRTEM image and the SAD pattern of the nanodiamond sample annealed for 1.5 h at the annealing temperature of 1350°C in a vacuum of 1 Pa. Figure 8(a) shows the HRTEM image of the nanodiamond sample annealed at the temperature of 1350°C. It is clear that all the a-C were transformed completely into the OLC after annealing the nanodiamond at the temperature of 1350°C. The OLC particles took on diverse shapes, such as quasi-spherical, elliptical, polyhedral and deformed onions. Some onions were found to be enclosed with linked external layers. The number of the onion graphitic shells ranged from several to 12 layers. The spacing of the observed lattice fringe was 0.344 nm, which was close to that of the (0 0 2) planes of the graphite. The SAD pattern of the sample is shown in Figure 8(b). The diffraction circles composed

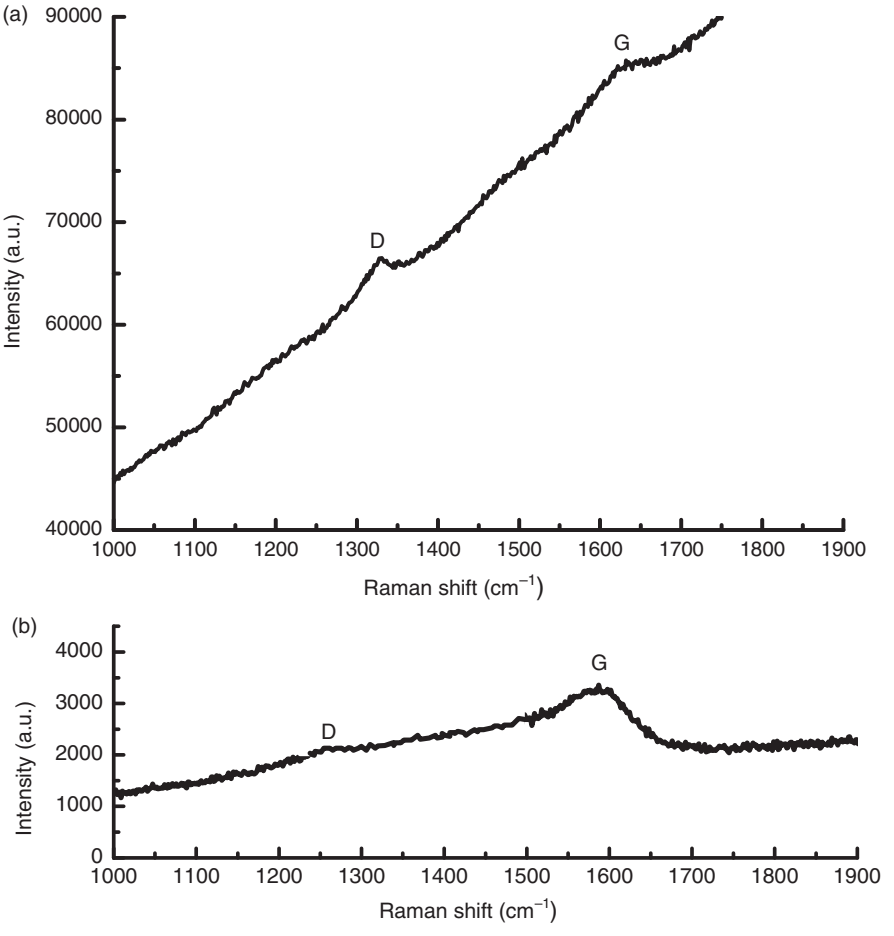

Figure 9. Raman spectra of the nanodiamond (a) and the OLC (b) annealed for 1.5 h at the temperature of 1350°C.

of the diffraction dot in Figure 8(b) corresponds to the diffraction of the nanographite (0 0 2), (1 0 0) and (1 1 0) planes, respectively, from the innermost to the outermost. From the SAD pattern of the sample shown in Figure 8(b), we can see that the a-C was completely transformed into the OLC after annealing the nanodiamond in the condition. This agreed very well with the HRTEM image result shown in Figure 8(a).

Figure 9 shows the Raman spectra of the nanodiamond and the OLC annealed for 1.5 h at the annealing temperature of 1350°C in a vacuum of 1 Pa in the wavenumber range from 1000 to 1900 cm^{-1}. From Figure 9(a), we can see that the deconvoluted spectrum included two peaks at approximately 1320 and 1600 cm^{-1}, respectively. The diamond peak at about 1320 cm^{-1} was downshifted and broadened with respect to the single crystal diamond peak at 1332 cm^{-1}. This downshift was thought to occur due to the particle size into the nanometre range. While the peak position at about 1660 cm^{-1} might come from the nanographite existing in the nanodiamond [44], which was downshifted from the

position 1572 cm^{-1} due to the influence of the structural defects. As shown in Figure 9(b), the peaks locating at about 1260 and 1580 cm^{-1}, respectively, resulted from the sp^3 and sp^2 structural carbons existing in the OLC, which demonstrated that the OLC was composed of the sp^2 structural carbon, as well as the sp^3 structural carbon.

The HRTEM images and the SAD patterns shown in Figures 1–8 suggest that the nanodiamond is transformed into the a-C gradually at first. Then, the a-C is gradually transformed into the OLC with an increase in annealing temperature. Moreover, at the annealing temperature of 600°C, the nanodiamond started transforming into a-C from the edge of the nanodiamond particle (1 1 1) crystal plane. At the annealing temperature of 750°C, the nanodiamond is completely transformed into the a-C. At the annealing temperature of 850°C, the a-C began transforming into the OLC at the edge area, which is lower by 350°C than that reported [45]. At the annealing temperature of 1000°C, the OLC particle with a size smaller than 5 nm is synthesised. However, in the centre of the OLC particle, the untransformed a-C coexisted. At the annealing temperature of 1100°C, the microstructure of the OLC particle with a size smaller than 5 nm is optimised. At the annealing temperature of 1200°C, the OLC particle with a size larger than 5 nm is fabricated. There is also untransformed a-C coexisting in the centre of the OLC particle. At the annealing temperature of 1350°C, all the a-C is transformed into the OLC. The average size of the OLC is approximately 5 nm, which is the same as that of the nanodiamond. The layers of the OLC varied from several to 12. As confirmed by the Raman spectra shown in Figure 9, the OLC is composed of the sp^3 and sp^2 structural carbons.

Many researchers have reported that the nanodiamond is first transformed into graphite from the nanodiamond's outmost (1 1 1) plane and then the graphite is gradually transformed into the OLC towards the centre [46,47]. However, in our research, we find that the nanodiamond is transformed into the a-C at first, and then the a-C is transformed into the OLC gradually with the increase in annealing temperature. Furthermore, the OLC particles can be fabricated at the annealing temperature of 850°C in our research because the vacuum of 1 Pa in our research is lower than that of the others' 10^{-2} Pa. We think that the oxygen in the vacuum chamber helps the formation of the OLC. However, future work is needed to be done to confirm the effect of oxygen on the OLC formation.

4. Conclusions

The OLC was synthesised by annealing detonation nanodiamond for 1.5 h in the vacuum of 1 Pa at the annealing temperature from 500°C to 1400°C. In order to know the transformation mechanism of the OLC by annealing the nanodiamond, an HRTEM and a Raman spectrometer were used to characterise the microstructures of the OLC comprehensively. The results showed that the nanodiamond was transformed into the a-C at first, and then the a-C was transformed into the OLC gradually, with the annealing temperature increase. At the annealing temperature of 600°C, the nanodiamond was transformed into the a-C from the nanodiamond particle edge. At the annealing temperature of 750°C, the nanodiamond was transformed into the a-C completely. At the annealing temperature of 850°C, the a-C was transformed into the OLC at the edge area. At the annealing temperature of 1000°C, the OLC particle with a size smaller than 5 nm was synthesised. At the annealing temperature of 1100°C, the OLC particle with a size

smaller than 5 nm was optimised. At the annealing temperature of 1200°C, the OLC particle with a size larger than 5 nm was fabricated. However, untransformed a-C coexisted in the centre of the OLC particle. At the annealing temperature of 1350°C, all the a-C was transformed into the OLC. The average size of the OLC was approximately 5 nm. The layers of the OLC varied from several to 12. The oxygen in the vacuum chamber helped the formation of the OLC.

References

[1] S. Iijima, *Direct observation of the tetrahedral bonding in graphitized carbon black by high resolution electron microscopy*, Cryst. Growth 50 (1980), pp. 675–683.

[2] V.Z. Mordkovich, A.G. Umnov, T. Inoshita, and M. Endo, *The observation of multiwall fullerenes in thermally treated laser pyrolysis carbon blacks*, Carbon 37 (1999), pp. 1855–1858.

[3] V.Z. Mordkovich, *The observation of large concentric shell fullerenes and fullerene-like nanoparticles in laser pyrolysis carbon blacks*, Chem. Mater. 12 (2000), pp. 2813–2828.

[4] A.F. Hebard, M.J. Rosseinsky, R.C. Haddon, D.W. Murphy, S.H. Glarum, T.T.M. Palstra, A.P. Ramirez, and A.R. Kortan, *Superconductivity at 18 K in potassium-doped C_{60}*, Nature 350 (1991), pp. 600–601.

[5] A. Hirate, M. Igarashi, and T. Kaito, *Study on solid lubricant properties of carbon onions produced by heat treatment of diamond clusters or particles*, Tribol. Int. 37 (2004), pp. 899–905.

[6] S.Y. Liu and S.Q. Sun, *Recent progress in the study of endohedral metallofullerenes*, J. Organomet. Chem. 599 (2000), pp. 75–86.

[7] P.J.F. Harris and S.C. Tsang, *Encapsulating uranium in carbon nanoparticles using a new technique*, Carbon (Letters to the Editor) 36 (1998), pp. 1859–1861.

[8] S. Barazzouk, S. Hotchandani, K. Vinodgopal, K. Vinodgopal, and P.V. Kamat, *Single-wall carbon nanotube films for photocurrent generation, a prompt response to visible-light irradiation*, J. Phys. Chem. B 108 (2004), pp. 17015–17018.

[9] G. Girishkumar, K. Vinodgopal, and P.V. Kamat, *Carbon nanostructures in portable fuel cells: Single-walled carbon nanotube electrodes for methanol oxidation and oxygen reduction*, J. Phys. Chem. B 108 (2004), pp. 19960–19966.

[10] D. Ugarte, *Graphitic nanoparticles*, MRS Bull. 19 (1994), pp. 39–42.

[11] S. Seraphin, D. Zhou, and J. Jiao, *Filling the carbon nanocages*, J. Appl. Phys. 80 (1996), pp. 2097–2104.

[12] N. Sano, H. Wang, I. Alexandrron, M. Chhowalla, K.B.K. Teo, G.A.J. Amaratunga, and K. Iimura, *Properties of carbon onions produced by an arc discharge in water*, J. Appl. Phys. 92 (2002), pp. 2783–2788.

[13] H. Lange, M. Sioda, A. Huczko, Y.Q. Zhu, H.W. Kroto, and D.R.M. Walton, *Carbon production by arc discharge in water*, Carbon 41 (2003), pp. 1617–1623.

[14] M. Ishigami, C. John, A. Zettl, and S. Chen, *A simple method for the continuous production of carbon nanotubes*, Chem. Phys. Lett. 319 (2000), pp. 457–459.

[15] N. Sano, H. Wang, M. Chhowalla, L. Alexandrou, and G.A.J. Amaraunga, *Synthesis of carbononion in water*, Nature 414 (2001), pp. 506–507.

[16] D. Ugarte, *Curling and closure of graphitic networks under electron beam irradiation*, Nature 359 (1992), pp. 707–709.

[17] D. Ugarte, *Morphology and structure of graphitic soot particles generated in arc-discharge C_{60} production*, Chem. Phys. Lett. 198 (1992), pp. 596–602.

[18] D. Ugarte and W.A. de Heer, *Generation of graphitic onions*, *Springer Series in Solid State Sciences*, Vol. 117, pp. 73–83.

[19] F. Banhart and P.M. Ajayan, *Carbon onions as nano-scopic pressure cells for diamond formation*, Nature 382 (1996), pp. 433–435.
[20] D. Golberg and Y. Bando, *Unique morphologies of boron nitride nanotubes*, Appl. Phys. Lett. 73 (1998), pp. 3085–3087.
[21] B.S. Xu and S.I. Tanaka, *Formation of a new electric material: Fullerene/metallic polycrystalline film*, Mater. Res. Soc. Symp. Proc. 472 (1997), pp. 179–182.
[22] F. Banhart, T. Failer, Ph. Redlich, and P.M. Ajayan, *The formation, annealing and self-compression of carbon onions under electron irradiation*, Chem. Phys. Lett. 269 (1997), pp. 349–335.
[23] B. Maquin, A. Derre, C. Labrugere, M. Trinquecoste, P. Chadeyron, and P. Delhaes, *Submicronic powders containing carbon, boron and nitrogen: Their preparation by chemical vapor deposition and their characterization*, Carbon 38 (2000), pp. 145–156.
[24] V. Serin, R. Brydson, A. Scott, Y. Kihn, O. Abidate, B. Maquin, and A. Derre, *Evidence for the solubility of boron in graphite by electron energy loss spectroscopy*, Carbon 38 (2000), pp. 547–554.
[25] N. Sano, H. Akazawa, T. Kikuchi, and T. Kanki, *Separated synthesis of iron-included carbon nanocapsules and nanotubes by pyrolysis of ferrocene in pure hydrogen*, Carbon 41 (2003), pp. 2159–2162.
[26] C.N. He, N.Q. Zhao, C.S. Shi, X.W. Du, and J.J. Li, *Carbon nanotubes and onions from methane deposition*, Mater. Chem. Phys. 97 (2006), pp. 109–115.
[27] S.H. Tsai, C.L. Lee, C.W. Chao, and H.C. Shih, *A novel technique for the formation of carbon-encapsulated metal nanoparticles on silicon*, Carbon 38 (2000), pp. 775–778.
[28] V.L. Kuznetsov, A.L. Chuvilin, Yu.V. Butenko, I.Y. Malkov, and V.M. Titov, *Onion-1ike carbon from ultra-disperse diamond*, Chem. Phys. Lett. 222 (1994), pp. 343–348.
[29] V.L. Kuznetsov, A.L. Chuvilin, E.M. Moroz, V.N. Kolomiichuk, S.K. Shaikhutdinov, and Y.V. Butenko, *Effect of explosion conditions on the structure of detonation soots: Ultradisperse diamond and onion carbon*, Carbon 32 (1994), pp. 873–882.
[30] S. Tomita, A. Burian, J.C. Dore, D. LeBolloch, M. Fujii, and S. Hayashi, *Diamond nanoparticles to carbon onions transformation: X-ray diffraction studies*, Carbon 40 (2002), pp. 1469–1474.
[31] D. Ugarte and W.A. Heer de, *Carbon onions produced by heat treatment of carbon soot and their relation to the 217.5 nm interstellar absorption feature*, Chem. Phys. Lett. 207 (1993), pp. 480–486.
[32] J.Y. Huang, H. Yasuda, and H. Mori, *Highly curved carbon nanostructures produced by ball-milling*, Chem. Phys. Lett. 303 (1999), pp. 130–134.
[33] B. Bokhonov and M. Korchagin, *The formation of graphite encapsulated metal nanoparticles during mechanical activation and annealing of soot with iron and nickel*, J. Alloys Compd. 333 (2002), pp. 308–320.
[34] T. Cabioc'h, M. Jaouen, E. Thune, P. Guérin, C. Fayoux, and M.F. Denanot, *Carbon onions formation by high-dose carbon ion implantation into copper and silver*, Surf. Coat. Technol. 128–129 (2000), pp. 43–50.
[35] W.Z. Wu, Z.P. Zhu, Y.I. Xie, J. Zhang, and T.D. Hu, *Preparation of carbon encapsulated iron carbide nanoparticles by an explosion method*, Carbon 41 (2003), pp. 317–321.
[36] M. Bustrzejewski, M. Sioda, and A. Huczko, *Nanocarbon production by arc discharge in water*, Carbon 41 (2003), pp. 1617–1623.
[37] L.G. Bulusheva, A.V. Okotrub, V.L. Kuznetsov, and D.V. Vyalikh, *Soft X-ray spectroscopy and quantum chemistry characterisation of defects in onion-like carbon produced by nanodiamond annealing*, Diamond Relat. Mater. 16 (2007), pp. 1222–1226.
[38] Z.J. Qiao, J.J. Li, N.Q. Zhao, C.S. Shi, and P. Nash, *Graphitisation and microstructure transformation of nanodiamond to onion-like carbon*, Scr. Mater. 54 (2006), pp. 225–229.

[39] O.O. Mykhaylyk and Y.M. Solonin, *Transformation of nanodiamond into carbon onions: A comparative study by high-resolution transmission electron microscopy, electron energy-loss spectroscopy, X-ray diffraction, small-angle X-ray scattering, and ultraviolet Raman spectroscopy*, J. Appl. Phys. 97 (2005), pp. 074302.1–074302.16.
[40] N.R. Greiner, *Diamonds in detonation soot*, Nature 333 (1998), pp. 440–442.
[41] V.L. Kuznetsov, I. Yu. Malkov, and A.L. Chuvilin, *Effect of explosion conditions on the structure of detonation soots: Ultradisperse diamonds and onion carbon*, Carbon 32 (1994), pp. 873–882.
[42] V.V. Danilenko, *Diamond synthesis and sintering by explosion*, Energoatomizdat, Moscow, 2003.
[43] V.Y. Dolmatov, *Detonation synthesis of ultradispersed diamonds: Properties and applications*, Russ. Chem. Rev. 70 (2001), pp. 607–626.
[44] A.C. Ferrari and J. Robertson, *Interpretation of Raman spectra of disordered and amorphous carbon*, Phys. Rev. B 61 (2000), pp. 14095–14107.
[45] V.L. Kuznetsov, Y.V. Butenko, A.L. Chuvilin, A.L. Romanenko, and A.V. Okotrub, *Electrical resistivity of graphitized ultra-disperse diamond and onion-like carbon*, Chem. Phys. Lett. 336 (2001), pp. 397–404.
[46] C.Z. Wang, K.M. Ho, and M.D. Shirk, *Laser-induced graphitization on a diamond (111) surface*, Phys. Rev. Lett. 85 (2000), pp. 4092–4095.
[47] A.S. Barnard, S.P. Russo, and I.K. Snook, *Structural relaxation and relative stability of nanodiamond morphologies*, Diamond Relat. Mater. 12 (2003), pp. 1867–1870.